DEX1, a Novel Plant Protein, Is Required for Exine Pattern Formation during Pollen Development in Arabidopsis[1]

Dawn M. Paxson-Sowders[2], Craig H. Dodrill, Heather A. Owen[3], and Christopher A. Makaroff*

Department of Chemistry and Biochemistry, Miami University, Oxford, Ohio 45056

To identify factors that are required for proper pollen wall formation, we have characterized the T-DNA-tagged, *dex1* mutation of Arabidopsis, which results in defective pollen wall pattern formation. This study reports the isolation and molecular characterization of *DEX1* and morphological and ultrastructural analyses of *dex1* plants. *DEX1* encodes a novel plant protein that is predicted to be membrane associated and contains several potential calcium-binding domains. Pollen wall development in *dex1* plants parallels that of wild-type plants until the early tetrad stage. In *dex1* plants, primexine deposition is delayed and significantly reduced. The normal rippling of the plasma membrane and production of spacers observed in wild-type plants is also absent in the mutant. Sporopollenin is produced and randomly deposited on the plasma membrane in *dex1* plants. However, it does not appear to be anchored to the microspore and forms large aggregates on the developing microspore and the locule walls. Based on the structure of DEX1 and the phenotype of *dex1* plants, several potential roles for the protein are proposed.

The pollen grain wall is architecturally and compositionally complex, and relatively little is known about the mechanisms that govern these two characteristics. The pollen wall consists of two layers: the outer exine layer, and the inner intine layer (Fig. 1). The intine is a relatively simple layer comprised of cellulose, pectin, and various proteins (Brett and Waldron, 1990). Although the exine pattern varies between species, in general it is divided into two main layers: an outer sculpted layer, the sexine, and an inner layer, the nexine (for review, see Stanley and Linskens, 1974). The exine is mainly composed of sporopollenin, which is responsible for many properties of the pollen wall, including physical strength and resistance to nonoxidative chemical, physical, and biological treatments, including fungal and bacterial attack (Heslop-Harrison, 1976; Meuter-Gerhards et al., 1999). Sporopollenin appears to be composed mainly of simple aliphatic polymers containing aromatic or conjugated side chains (Ahlers et al., 1999). However, its exact composition is unknown and may vary between species (Meuter-Gerhards et al., 1999). The patterning of sporopollenin is responsible for the elaborately sculpted, complex structures of pollen walls (Erdtman, 1952). The reticulate pollen wall pattern, which is made up of a series of ridges, muri, and spaces, lumina, is sculpted in a taxonomic-specific manner (Erdtman, 1969).

In addition to being highly ornate and serving as a protective barrier for the pollen grain, the exine is also involved in cell-to-cell recognition. Factors responsible for recognition and subsequent interactions between the pollen grain and the stigmatic surface during fertilization are localized to the outer exine layer of the pollen wall (Heslop-Harrison, 1976; Nasrallah and Nasrallah, 1989; Zinkl et al., 1999). Initial interactions between the pollen grain and the stigmatic surface are potentially dependent upon adhesion molecules located within the exine (Zinkl et al., 1999).

There have been numerous studies describing pollen wall development and exine patterning for a large number of species (for review, see Cutter, 1971; Heslop-Harrison, 1971b; Stanley and Linskens, 1974; Blackmore and Barnes, 1990; Scott, 1994). However, factors that establish the patterning have not yet been identified. No observable wall structures exist during meiosis, although centrifugation experiments suggest that pattern determinants are present in the cytoplasm of the microsporocyte by late prophase I (Sheldon and Dickinson, 1983). Numerous structures have been implicated in wall formation, including the primexine matrix, microtubules, endoplasmic reticulum (ER), and the plasma membrane. The primexine matrix, the first pollen wall material laid down during wall development, has long been thought to play an important role in the final exine pattern (Heslop-Harrison, 1963; Rowley and Skvarla, 1975; Fitzgerald and Knox, 1995). Microtubules have been implicated in the movement of wall material to the surface of the microspore (Perez-Munoz et al., 1995). The ER may be involved in determining the

[1] This work was supported by the U.S. Department of Agriculture (grant no. 95–37304–2246) and by the National Research Initiative Competitive Grants Program (to C.A.M.).

[2] Present address: Department of Rheumatology, Children's Hospital Medical Center, Cincinnati, OH 45229.

[3] Present address: Department of Biological Sciences, University of Wisconsin, Milwaukee, WI 53211.

* Corresponding author; e-mail: makaroca@muohio.edu; fax 513–529–5715.

Article, publication date, and citation information can be found at www.plantphysiol.org/cgi/doi/10.1104/pp.010517.

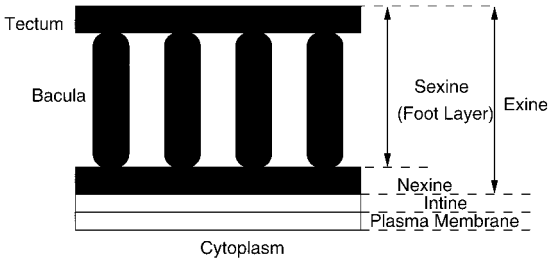

Figure 1. General pollen wall structure. Schematic representation of the main features of a mature pollen grain wall. The innermost layer adjacent to the plasma membrane is the intine. The exine is comprised of the sexine and nexine, a continuous layer covering the entire pollen grain. The bacula and tectum make up the sculpted sexine in this representation.

location of the colpi, regions of pollen tube outgrowth (Dickinson and Sheldon, 1986; Perez-Munoz et al., 1995). Other studies have suggested that the final reticulate pattern of the pollen wall results from an invagination of the plasma membrane to resemble the final pattern (Takahashi, 1989; Takahashi and Skvarla, 1991). Therefore, although circumstantial evidence exists for the involvement of numerous factors in pattern formation, direct evidence supporting the role of any particular factor has been difficult to obtain.

An ultrastructural comparison of pollen wall development between wild-type Arabidopsis and *dex1* plants, a T-DNA-tagged, pollen wall mutant, suggested that the plasma membrane does play an integral role in pollen wall pattern formation (Paxson-Sowders et al., 1997). The *dex1* mutation was found to block the normal patterning of the plasma membrane and disrupt sporopollenin deposition leading to pollen grain collapse. Wall development in the mutant resembled wild type until early tetrad stage, when in wild-type plants the plasma membrane adopted a regular undulating pattern. The plasma membrane of mutant plants lacked this regular patterning. Sporopollenin was synthesized and deposited in the mutant, but did not appear to be anchored to the surface of the microspore. This analysis suggested that DEX1 might serve as the nucleation point for sporopollenin deposition.

To better understand the role of DEX1 in pollen wall formation, we have conducted a more detailed analysis of *dex1* plants and isolated and characterized the *DEX1* gene. DEX1 appears to be a novel plant protein that exhibits limited sequence similarity to hemolysin and animal α integrins and is predicted to bind calcium. Analysis of pollen wall development in *dex1* plants suggests that the mutation disrupts normal primexine development, which ultimately affects the conformation of the membrane and sporopollenin deposition. The phenotype of mutant plants and the structure of DEX1 raise several possibilities for its role in the cell.

RESULTS

Isolation and Characterization of the *dex1* Locus

Genetic and Southern-blot analyses were conducted to determine whether the T-DNA insert is linked with the *dex1* mutation. The results from a genetic analysis of four generations (F_4–F_7) of *dex1* plants are shown in Table I. Segregation data (fertile: sterile) from unselected plants (seeds sown directly on to soil) indicated that *dex1* is inherited in a simple recessive manner, whereas segregation of kanamycin resistance indicated the presence of a single expressed T-DNA insert. Kanamycin-resistant seedlings segregate 2:1 (fertile:sterile) consistent with linkage of the *dex1* mutation and T-DNA insert.

Results from Southern-blot analyses corroborated linkage between the mutation and T-DNA insert. Sterile, unselected *dex1* plants contain two *Hin*dIII fragments (5.6 and 3.3 kb) that hybridized to left border (LB) probes and one fragment (4.6 kb) that hybridized with right border (RB) probes (data not shown). These results suggested that the *dex1* insertion site contains two T-DNAs inverted about the RB (Fig. 2A). Identical results were obtained from over 60 sterile plants spanning three generations, confirming cosegregation between the T-DNA and *dex1* mutation and demonstrating that no silent inserts are present in *dex1* plants.

Plant DNA flanking the T-DNA insertion site was isolated from a *dex1* λ library. Two classes of clones containing LB plant junctions were identified and characterized. One class contained a 2.7-kb *Hin*dIII/*Eco*RI fragment adjacent to the LB, whereas the other contained a 3.0-kb *Sac*I fragment containing plant DNA and a partial T-DNA LB. Southern-blot analysis indicated that the fragments represent both sides of a single T-DNA insertion site (data not shown).

When northern blots of bud poly(A^+) RNA from wild-type and *dex1* plants were probed with the 2.7-kb *Hin*dIII/*Eco*RI and 3.0-kb *Sac*I fragments, a 3,100-nucleotide (nt) transcript was detected in wild-type RNA that was absent in RNA from *dex1* plants (Fig. 3A). Equal loading of RNA was confirmed by reprobing the blot with *ACT8* (An et al., 1996; data

Table I. *Kanamycin and male sterility segregation ratios of dex1 plants*

The lines represent progeny from four generations of kanamycin-resistant plants derived from a cross between a sterile *dex1* plant and a wild-type (Wassilewskija) plant. Kan^R, Kanamycin resistant; Kan^S, kanamycin sensitive. Segregation ratios are shown in parentheses.

Generation	Fertile:Sterile[a]	Kan^R:Kan^S	Fertile Kan^R:Sterile Kan^R
F_4	163:55 (3.0:1)	342:116 (2.9:1)	103:41 (2.5:1)
F_5	115:32 (3.6:1)	244:92 (2.7:1)	121:54 (2.2:1)
F_6	255:69 (3.6:1)	704:203 (3.5:1)	149:53 (2.8:1[b])
F_7	76:23 (3.3:1)	900:283 (3.2:1)	95:38 (2.5:1)

[a] Unselected seed, not scored for kanamycin resistance. [b] Chi-squared test $0.05 > P > 0.01$; all others $P > 0.05$.

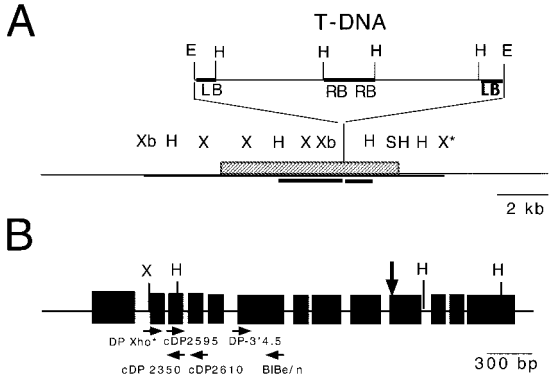

Figure 2. Map of the *DEX1* locus and exon patterns. A, Map of a 10-kb region of chromosome 3. The extent of the *DEX1* coding region (shaded box) is shown relative to the region used in the complementation experiments (medium black line). Heavy black lines represent regions that hybridized to LB and RB probes. Restriction sites shown are: H, *Hin*dIII; E, *Eco*RI; X, *Xho*I; and Xb, *Xba*I. X* is an *Xho*I site that is derived from λ DNA and was used for cloning the complementation clone. B, Partial restriction map and exon pattern of *DEX1*. The positions of exons are shown as solid boxes. The position and direction of primers used in this study are shown as horizontal arrows below the map. The position of the T-DNA insertion site is shown as a vertical arrow. Restriction sites are as in A.

not shown). These results indicated that the T-DNA inserted into a gene and disrupted its expression. Therefore, a detailed analysis of the T-DNA insertion site was conducted.

Molecular Analysis of DEX1

Genomic and cDNA sequences were isolated and characterized. A 1,938-bp cDNA clone that maps to both sides of the T-DNA insertion site was obtained from the PRL-2 cDNA library. Sequence analysis of the clone indicated that it contained a long, open reading frame (ORF) that was not homologous to any known gene. The discrepancy between the size of the clone, 1,938 bp, and the 3,100-nt transcript detected in northern blots suggested that the clone encoded a partial cDNA. Therefore, genomic clones were isolated and characterized. Three positive clones, which spanned approximately 28 kb, were identified; two of the clones were identical and overlapped the third by 4.7 kb around the T-DNA insertion site.

Complementation experiments were conducted to ensure that *DEX1* was correctly identified as the gene responsible for the male sterility phenotype. *Agrobacterium tumefaciens* cells containing a 10.2-kb *Xba*I-*Xho*I *DEX1* genomic fragment (Fig. 2A) in pPZP121 was used to transform a segregating population of *dex1* plants. Thirty gentamycin-resistant plants representing at least five transformation events were identified. All the plants contained the gentamycin gene as expected and were fertile. Progeny from two of the original 30 lines (lines 6 and 17) were completely kanamycin resistant, indicating that they are homozygous for the *dex1* mutation (Table II). Both lines segregated for the sterility phenotype, consistent with complementation of the *dex1* mutation by the 10.2-kb *Xba*I-*Xho*I fragment. PCR analysis of progeny from lines 6 and 17 showed that all sterile plants lacked the complementation construct, whereas all gentamycin-resistant plants were fertile as expected. Data from the analysis of seven additional lines, which segregated for kanamycin resistance and were heterozygous for the *dex1* mutation, were also consistent with complementation by the clone (Table II). Progeny from five of the seven lines were completely fertile, indicating that the mutation had been complemented; two lines produced some sterile plants, indicating that they are most likely segregating for the complementation construct. These results clearly demonstrate that fertility was restored to *dex1* plants by the 10.2-kb fragment containing the *DEX1* gene.

DNA sequence analysis of approximately 7.4 kb of wild-type genomic DNA surrounding the T-DNA insert was conducted. These results confirmed exons that correspond to the cDNA and identified several predicted exons. Reverse transcriptase (RT)-PCR and inverse PCR (IPCR) experiments were used to isolate a 3,112-bp, full-length *DEX1* cDNA (Fig. 4), which is comparable to the predicted 3,100-nt transcript size.

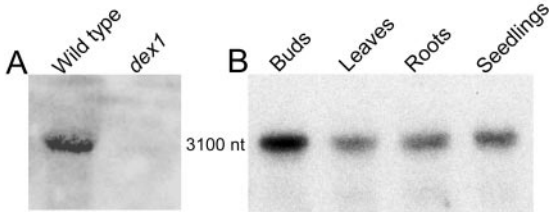

Figure 3. DEX1 expression analysis. A, Northern blot of poly(A^+) RNA, isolated from buds of wild-type and *dex1* mutant plants probed with a mixture of the 2.7-kb *Hin*dIII/*Eco*RI fragment 1 and the 3.0-kb *Sac*I fragment. B, Northern blot of total RNA isolated from wild-type buds, leaves, roots, and seedlings, was probed with the partial *DEX1* cDNA clone. Equal loadings were determined by subsequent hybridization with an rRNA probe.

Table II. *Results from dex1 complementation experiments*

The lines represent the progeny from gentamycin-resistent plants obtained from infiltration of a segregating population of *dex1* plants with a *DEX1* complementation clone. Kan^R, Kanamycin resistant; Kan^S, kanamycin sensitive.

Family	Kan^R:Kan^S	Fertile:Sterile[a]
1	314:124	28:0
4	239:60	24:0
5	166:35	30:0
7	220:58	50:8
10	297:79	31:0
12	49:18	27:1
14	201:59	31:0
6	185:0	38:10
17	222:0	25:17

[a] Seeds were selected for kanamycin resistance prior to transfer to soil.

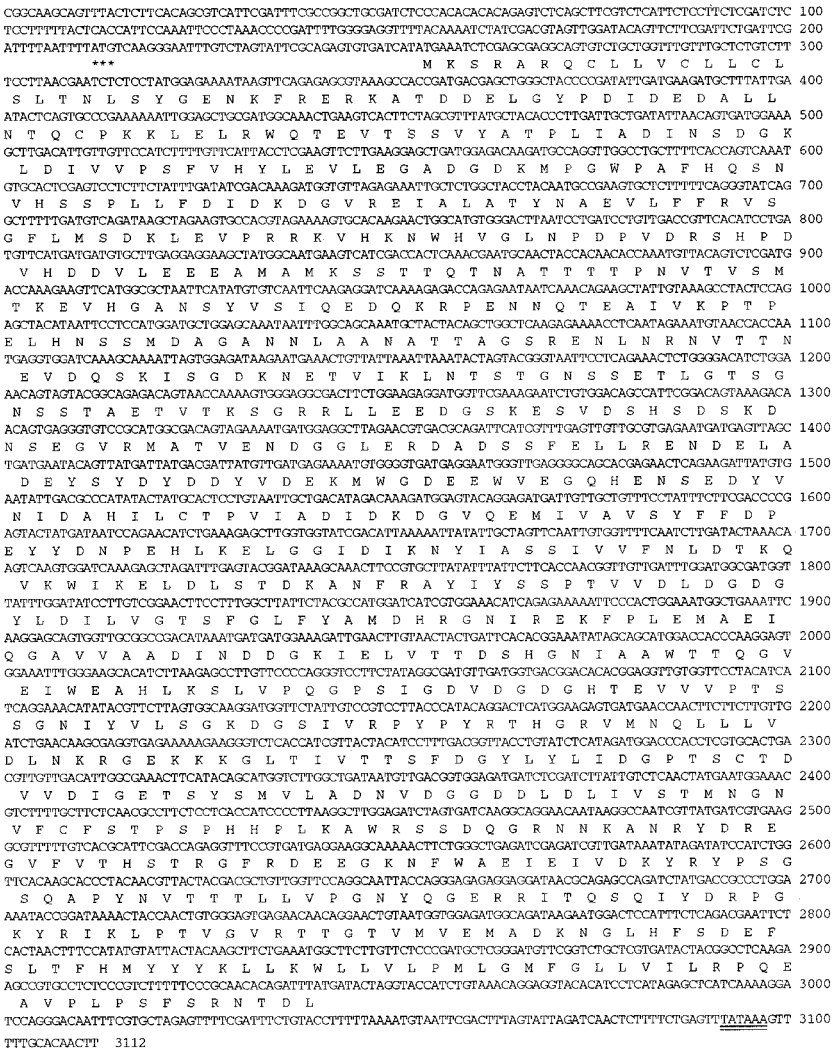

Figure 4. DEX1 cDNA and deduced amino acid sequence. The deduced DEX1 amino acid sequence is shown below the cDNA sequence. The 5′ end of the cDNA sequence shown is the longest clone obtained by IPCR. A potential polyadenylation signal is double underlined. The upstream AUG is marked with asterisks.

Alignment of cDNA and genomic sequences indicated that the *DEX1* transcript is encoded by 13 exons and spans 5.05 kb (Fig. 2B). The T-DNA inserted in the 5′ end of exon 9. The *DEX1* transcript is predicted to have a 172-bp 3′-untranslated region, excluding the poly(A^+) tail. A consensus AAUAAA-like polyadenylation signal is present at position 3,092, 15 bases upstream of the poly(A^+) tail. The cDNA does not, however, contain a UG-rich consensus element, which is required for the efficient utilization of the poly(A^+) signal in several genes (Wu et al., 1995).

The 5′ end of the transcript was mapped 255 bp 5′ to the start of translation. The 5′-untranslated region is considerably longer than that found in most plant genes, which typically contain about 100 nucleotides (Futterer and Hohn, 1996). The predicted *DEX1* translation start site is not the 5′ most proximal AUG in the transcript. Another potential translation start site is present 38 bp upstream of that predicted for *DEX1*. The upstream ORF (uORF) terminates before the putative *DEX1* initiation site. Furthermore, *DEX1* lacks the AUG context consensus sequence [caA(A/C) a*AUG*GCg], which is thought to be important for AUG codon recognition (Joshi et al., 1997). The effect of the uORF on *DEX1* translation is unknown; however, the presence of a uORF and a poor AUG context suggests that *DEX1* could be the subject of translational regulation (Futterer and Hohn, 1996; Joshi et al., 1997).

The predicted DEX1 protein is 896 amino acids long with a mass of 99.8 kD and a pI of 4.61. The protein is mainly hydrophilic, containing large numbers of polar (28%) and charged (33%) amino acids, except for the amino and carboxy termini, which are relatively hydrophobic. Analysis of DEX1 with Prediction of Protein Sorting Signals and Localization Sites in Amino Acid Sequences (Horton and Nakai, 1996) predicts that the first 22 amino acids denote a cleavable signal sequence, whereas amino acids 860 through 880 could represent a transmembrane domain. DEX1 is predicted to be a type 1a membrane protein, which is favored for plasma membrane proteins.

DEX1 is not homologous to any previously characterized protein. It does, however, show limited sequence similarity to a small number of proteins, including a hemolysin-related protein from *Vibrio cholerae* (10.5% over the length of the protein). An approximately 200-amino acid segment of DEX1 also shows limited similarity (24% identity over residues 439–643) to the calcium-binding domain of animal α-integrins (Palmer et al., 1993). In this region are at least two sets of putative calcium-binding ligands, which are also present in a predicted Arabidopsis *calmodulin* protein (AC009853). Therefore, DEX1 may bind calcium.

A northern-blot analysis was conducted to determine whether *DEX1* expression is restricted to buds. When the *DEX1* cDNA was used to probe a northern blot containing wild-type bud, leaf, root, and seedling total RNA, a signal corresponding to a 3,100-nt transcript was detected in all tissue (Fig. 3B). DEX1 transcripts may be present at slightly higher levels in buds, but the transcript is clearly present in all four samples. Therefore, *DEX1* appears to be expressed at low, relatively equal amounts throughout the plant.

Morphological Studies

A prior analysis of *dex1* plants suggested that the mutant phenotype was restricted to developing microspores (Paxson-Sowders et al., 1997). However, the observation that *DEX1* is expressed throughout the plant raised the possibility that other abnormalities may be present in *dex1* plants. Therefore, various aspects of plant development were analyzed in *dex1* plants, including plant height, number of axial branches, leaf size and number, root shape, and growth rate. No statistically significant differences were identified between wild-type and *dex1* plants in any of the analyses conducted (data not shown). Therefore, although DEX1 transcripts are present throughout wild-type plants, no other gross morphological defects were identified in *dex1* plants. We cannot, however, eliminate the possibility that subtle alterations have gone undetected.

Morphological characteristics of anther cells, from meiosis to approximately the ring vacuolate stage, were also examined in *dex1* plants. No differences were detected in microsporocytes during meiosis or in any of the four anther cell layers (epidermis, endothecium, middle layer, and tapetum) during microsporogenesis and microgametogenesis (data not shown). Aniline blue staining of semithin sections also revealed apparently normal callose production. The only noticeable defect was the previously described alteration in sporopollenin distribution during the late tetrad and early released microspore stages.

In a previous transmission electron microscopy study of pollen wall formation in *dex1* plants using samples prepared by chemical fixation, we found that the mutation blocks the normal invagination of the plasma membrane following primexine production and the proper deposition of sporopollenin (Paxson-Sowders et al., 1997). It has been shown that rapid freezing followed by freeze substitution leads to better preservation of the tissue and the elimination of artifacts sometimes seen in chemically fixed samples, in particular in membranes and the cytoskeletal elements (Kiss et al., 1990; Kiss and Staehelin, 1995). Therefore, we reanalyzed pollen wall formation in *dex1* plants using samples prepared by high-pressure freezing followed by freeze substitution. A total of 53 blocks containing wild-type anthers (10 at tetrad stage) and 73 blocks containing *dex1* anthers (24 at tetrad stage) were analyzed.

Pollen wall development in *dex1* plants resembled wild-type development up to primexine formation. In wild-type plants, the primexine is first evident as discrete electron-dense deposits in the callose wall directly outside the microspore membrane at early tetrad stage (Fig. 5A). Later in development, portions of the microspore membrane display regular undulations, although other portions of the plasma membrane are straight. Variations are observed in both thickness and electron density of the primexine at this stage, with the thickest and most electron-dense areas located within the membrane undulations (Fig. 5B). Similar electron-dense regions have been observed in *Brassica campestris* and referred to as spacers (Fitzgerald and Knox, 1995). Later in development, the microspore membrane becomes straight and the primexine matrix has thickened (Fig. 5C). Electron-dense deposits of material (potentially sporopollenin) are present within the primexine matrix adjacent to the callose wall. They are not initially in contact with the microspore membrane. By late tetrad stage, electron-dense material within the primexine matrix is clearly recognizable as the developing exine. Fine fibrillar material is present in the primexine matrix. In contrast to observations in chemically fixed material (Paxson-Sowders et al., 1997), the probaculae do not make direct contact with the microspore membrane until later in wall development (Fig. 5D).

As observed in wild-type plants, primexine is first evident as discrete electron-dense deposits directly outside the microspore membrane within the callose wall of *dex1* plants (Fig. 5E). The first detectable difference in *dex1* plants is that the plasma membrane does not form the undulations seen in wild-type plants (Fig. 5F). Because this stage of wall development is relatively short-lived, it is possible that the *dex1* microspore membranes may form some undulations; however, given the relatively large number of samples examined in this study, if it does occur, it is a rare event. Abnormalities begin to appear in the primexine at approximately the same time as alterations are detected in the plasma membrane (Fig. 5F). The primexine never forms a uniform layer of elec-

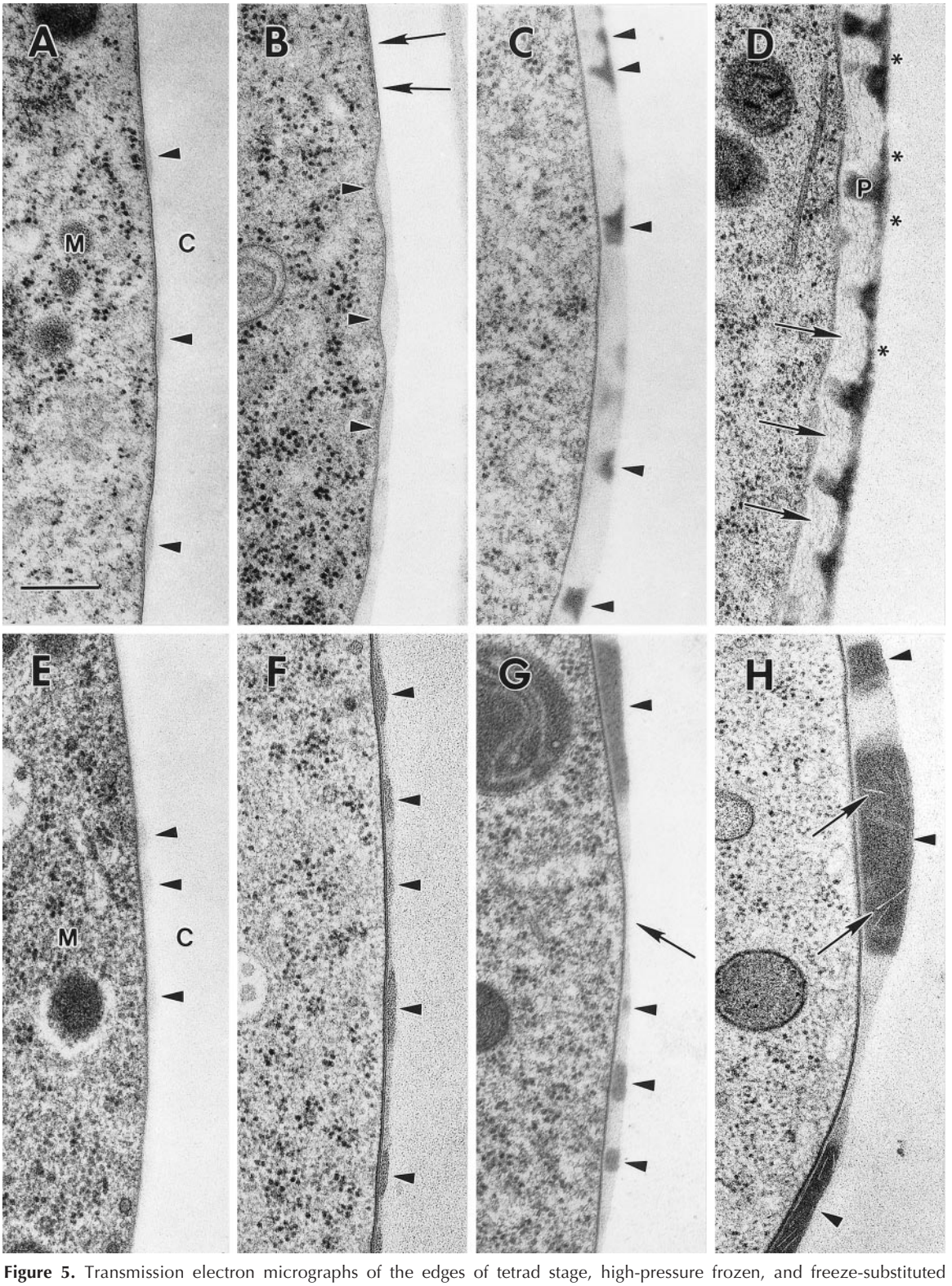

Figure 5. Transmission electron micrographs of the edges of tetrad stage, high-pressure frozen, and freeze-substituted microspores of Arabidopsis. All micrographs are shown at equal magnifications. Size bar = 0.25 μm. A through D, Developmental series of WT microspores. A, Within the callose wall (C), primexine is first evident as discrete electron-dense deposits (arrowheads) directly outside the microspore (M) membrane. B, Later in development, portions of the microspore plasma membrane display regular undulations (arrowheads), although other portions of the plasma membrane are straight (arrows). The primexine varies in both thickness and electron density at this stage, with the thickest and most electron-dense areas located within the membrane undulations. C, Later in development the primexine matrix has increased in thickness

(*Legend continues on facing page.*)

tron lucent material, rather lens-shaped, electron-dense areas are observed with more electron-lucent regions between them (Fig. 5G). At this level of analysis, it is difficult to conclude with certainty if the more electron-lucent regions in the primexine of wild-type and *dex1* plants represent the same material. However, based on the shape and relative electron densities, we believe that they are, in fact, different. Later in development, regions of electron-dense deposits were observed in contact with the callose wall and in some instances the microspore membrane (Fig. 5H). Linear, electron-lucent regions are observed within some of the electron-dense deposits.

Therefore, results from samples prepared by rapid freezing followed by freeze substitution identified the following alterations in *dex1* pollen wall formation: (a) Rippling of the microspore membrane during early primexine deposition does not appear to occur. (b) Primexine deposition is delayed and altered; spacers do not form. (c) Sporopollenin deposition occurs randomly along the microspore wall. (d) Fibrillar material is not present in the primexine. The membrane patterning and sporopollenin deposition at the peaks of the membrane previously observed after primexine deposition in chemically fixed, wild-type plants (Paxson-Sowders et al., 1997) was not observed in these better preserved preparations.

DISCUSSION

Pollen grain wall formation represents an interesting but poorly understood aspect of pollen development. Although the physical properties and functions of the pollen wall have been described in detail (Erdtman, 1952; Skvarla and Larson, 1966; Cutter, 1971; Heslop-Harrison, 1971b, 1976; Scott, 1994; Knox and Suphioglu, 1996; Toriyama et al., 1998; El-Ghazaly et al., 1999), little is known about how the pollen wall is actually formed. To better understand this important process, we present the results of detailed molecular and morphological studies of a T-DNA-tagged, male-sterile line of Arabidopsis that is defective in pollen wall development. Molecular analysis of *dex1* plants shows that the gene is tagged with a T-DNA and that no silent inserts are present in the line. A full-length *DEX1* cDNA has been isolated through library screening, RT-PCR, and IPCR. The 3,112-nt *DEX1* transcript is absent in mutant RNA, and *DEX1* genomic sequences are able to complement the *dex1* mutation, confirming that *DEX1* encodes the gene responsible for the male sterility phenotype.

DEX1 encodes an 896-amino acid protein that is predicted to localize to the plasma membrane, with residues 1 through 860 being located outside of the cell, residues 880 through 895 on the cytoplasmic side of the membrane, and amino acids 861 through 879 representing a potential membrane spanning domain. Twelve potential N-glycosylation sites are present in DEX1. Therefore, the protein has the potential to be heavily modified and interact with the cell wall. Further experiments are required to evaluate these predictions.

DEX1 appears to be a unique plant protein; homologs are not present in bacteria, fungi, or animals. DEX1 shows the greatest sequence similarity to a hemolysin-like protein from *V. cholerae,* whereas an approximately 200-amino acid segment of DEX1 (amino acids 439–643) also shows limited similarity to the calcium-binding domain of α-integrins. In this region are at least two sets of putative calcium-binding ligands that are also present in a predicted Arabidopsis *calmodulin* protein (AC009853). Therefore, it appears that DEX1 may be a calcium-binding protein.

Our analysis of pollen wall development has identified several alterations in *dex1* plants: (a) Rippling of the microspore membrane during early primexine deposition does not occur; (b) Primexine deposition is delayed, reduced in thickness, and apparently altered in conformation; (c) Spacers do not form in the primexine, which results in sporopollenin deposition randomly along the microspore wall; (d) Sporopollenin never becomes attached to the microspore, and the pollen wall does not form. These results suggest

Figure 5. (*Legend continued from facing page.*)
and is evenly distributed along the surface of the straight microspore membrane. Electron-dense deposits of material have formed within the primexine matrix (arrowheads). These deposits appear to be in contact with the wall on the callose-facing surface of the primexine matrix, but are not in contact with the membrane on the microspore-facing surface of the primexine matrix. D, At a later stage, electron-dense material within the primexine matrix is clearly recognizable as the developing exine. Fine fibrillar material (arrows) is evident in the primexine matrix between the probaculae (P), which are not in direct contact with the microspore membrane. The pattern of the future tectum has been established (asterisks) within the callose-facing surface of the primexine. E through H, Developmental series of *dex1* microspores. E, As in WT, primexine is first evident as discrete electron-dense deposits (arrowheads) directly outside the microspore (M) membrane within the callose wall (C). F, The primexine has increased slightly in thickness outside a straight microspore membrane. Areas of two different electron densities can be distinguished within the primexine. Regularly spaced along the microspore membrane, the more electron-dense areas (arrowheads) are lens shaped and thicker than the more electron-lucent regions between them. G, Later in development the primexine matrix has increased in thickness on some areas of the microspore, but in other areas is extremely thin (arrow). Electron-dense deposits of varying sizes (arrowheads) have formed within the primexine matrix. H, At a later stage the electron-dense deposits (arrowheads) and primexine that enclose them have become thicker. Linear electron-lucent regions (arrows) are present within some of the deposits.

that the *dex1* mutation disrupts normal primexine development, which ultimately affects the conformation of the membrane and sporopollenin deposition.

The alterations observed in *dex1* plants, as well as the predicted structure of DEX1, raise several possibilities for the role of the protein in pollen wall formation. (a) DEX1 could be a linker protein. It may associate with the microspore membrane and participate in attaching either the primexine or sporopollenin to the plasma membrane. Absence of the protein from the microspore surface could result in structural alterations in the primexine. The numerous potential N-glycosylation sites are consistent with attachment of DEX1 to the callose wall, the intine, or both. (b) DEX1 may be a component of the primexine matrix and play a role in the initial polymerization of the primexine. Changes in Ca^{+2} ion concentrations appear to be important for pollen wall synthesis; β-glucan synthase is activated by micromolar concentrations of Ca^{+2} during callose wall formation (Kudlicka and Brown, 1997). (c) DEX1 could be part of the rough ER and be involved in processing and/or transport of primexine precursors to the membrane. The delayed appearance and general alterations in the primexine are consistent with a general absence of primexine precursors. The primexine matrix is initially composed of polysaccharides, proteins, and cellulose, followed by the incorporation of more resistant materials (Heslop-Harrison, 1963, 1971a; Rowley and Southworth, 1967; Dickinson and Heslop-Harrison, 1977). Therefore, DEX1 may participate in the formation or transport of any number of different components. Based on our current understanding, we cannot distinguish between the various alternatives, but currently favor the possibility that DEX1 is a component of the primexine matrix or the ER and is involved in the assembly of primexine precursors.

A second unresolved question involves our finding that *DEX1* transcripts are present throughout wild-type plants, whereas disruption of pollen wall formation is the only morphological alteration identified in *dex1* plants. At this time, it is not clear if the DEX1 protein is present in vegetative tissues. Features associated with the 5′ end of *DEX1* transcripts raise the possibility that it may undergo translational regulation and that the DEX1 protein may not be produced in vegetative cells. The *DEX1* transcript is predicted to have a long 5′-untranslated region (255 bp), a uORF, and poor AUG context around the *DEX1* start site. Many genes identified as having a poor AUG context in higher plants correspond to tightly regulated proteins, including: transcription factors, signal transducers, regulatory proteins, metabolic enzymes, cell wall, and stress proteins (Joshi et al., 1997). Although the presence of uORFs is rare, there are several examples of plant transcripts that contain uORFs including *OPAQUE2,* a maize (*Zea mays*) transcription factor, the maize *Lc* transcriptional activator, and MEK1, a homolog of mitogen-activated protein kinase (Morris et al., 1997). In addition, several plant plasma membrane H^+-ATPase genes possess long 5′-untranslated regions and a uORF and appear to undergo translational regulation (Lukaszewicz et al., 1998).

If DEX1 is present in all tissues, it is possible that the *dex1* mutation results in alterations at the microscopic level that have so far gone undetected in our analyses. The lack of a readily observable phenotype upon the reduction of certain plant cell wall proteins has been observed previously. For example, transgenic tobacco (*Nicotiana tabacum*) plants that over and/or underexpress extensin exhibit essentially normal morphological and developmental profiles (Memelink et al., 1993). Likewise, the effect of the *dex1* mutation in whole plants might only be visible under specific growth conditions. Conversely, DEX1 may only be functionally active in developing pollen grains. This type of specific functionality has been seen in some regulatory proteins, which play specific roles in reproductive development but are expressed in vegetative as well as in reproductive tissue (Jofuku et al., 1994; Reiser et al., 1995; Klucher et al., 1996). A more detailed analysis of vegetative tissues is required to examine the distribution of DEX1 and determine whether other abnormalities exist in *dex1* plants.

In summary, this report presents the isolation and characterization of *DEX1*, a gene essential for early pollen wall formation. Plants containing the *dex1* mutation exhibit alterations in the microspore membrane and primexine formation, which prevent the normal deposition of sporopollenin. The sequence of the predicted DEX1 protein and the results of our ultrastructural studies suggest that that DEX1 may either be a component of the primexine matrix or the ER and involved in the assembly of primexine precursors. However, further experiments are needed to understand the specific role of the protein. Experiments to determine DEX1 localization patterns and the role it plays in vegetative cells are currently under way. These should provide further insight into the role of DEX1 in pollen wall pattern formation.

MATERIALS AND METHODS

Plant Material

Arabidopsis, ecotype Wassilewskija, was the source of both wild-type and mutant plants. The *dex1* mutation was isolated as a part of a large-scale screen of T-DNA seed transformants at the DuPont Company (Wilmington, DE). The male-sterile phenotype was determined by visual inspection of plants grown on a commercial potting mix in growth chambers at 20°C with a 16-/8-h light/dark cycle. Kanamycin resistance was used to monitor the segregation of T-DNA inserts (Feldmann and Marks, 1987). Buds, leaves, and siliques were harvested from mature plants. Roots and seedlings were harvested from seeds sown on

Murashige and Skoog medium plates (Murashige and Skoog, 1962). All samples were harvested, frozen in liquid N_2, and stored at −80°C until needed.

Microscopy

Plant material for semithin sections was prepared and embedded in Spurr's resin as previously described (Owen and Makaroff, 1995). Semithin sections (0.5 μm) were cut with a diamond knife on an Ultracut S microtome (Reichert, Leica Microsystems, Inc., Bannockburn, IL) and stained with Azure B (Hoefert, 1968). Aniline blue and Auramine O staining of semithin sections (Peirson et al., 1996) was used to determine the presence of callose and sporopollenin, respectively.

Plant material for ultrathin sections was prepared by high-pressure freezing and freeze substitution (Kiss and Staehelin, 1995). To enrich for meiosis and tetrad stage microspores, buds approximately 0.5 mm in length were removed from inflorescences, teased opened in 15% (w/v) dextran (M_r 38,000), and placed in specimen hats precoated with 3% (w/v) lecithin in chloroform and filled with 15% (w/v) dextran. Specimens were frozen with an HPM 010 high-pressure freezing apparatus (Bal-tec AG, Balzers, Liechtenstein). Following freezing, specimens were freeze substituted in 2% (v/v) OsO_4 in anhydrous acetone at −80°C for 5 d. The specimens were then placed at −20°C for 4 h, −4°C for 4 h, 4°C for 1 h, and room temperature for 2 h. After three exchanges of anhydrous acetone followed by three washes with anhydrous acetone, buds were infiltrated and embedded in Spurr's resin. Silver sections were cut with an MT 7000 ultramicrotome (RMC Products, Boeckeler Instruments, Inc., Tucson, AZ) and stained for 30 min in 0.5% (v/v) methanolic uranyl acetate followed by Reynold's lead citrate. Sections from 53 wild-type and 73 *dex1* blocks were viewed with an H-600 transmission electron microscope (Hitachi, Tokyo) operating at 75 kV.

Hybridizations

Approximately 10 μg of genomic DNA, isolated from individual plants (Doyle and Doyle, 1990), was subjected to Southern-blot analysis using [α-^{32}P]dATP-labeled probes. After hybridization and washing, the blots were analyzed using a phosphorimager (Molecular Dynamics, Sunnyvale, CA).

Total RNA was isolated from individual tissues using guanidine hydrochloride (Logemann et al., 1987). Poly(A^+) RNA was isolated using oligo(dT) cellulose (Jacobson, 1987). Northern blots containing 10 μg of total RNA or 3 μg of poly(A^+) RNA were prepared and hybridized with [α-^{32}P]dATP-labeled probes (Makaroff and Palmer, 1987). Hybridized blots were washed and viewed as described above.

Construction and Screening of Genomic and cDNA λ-Libraries

Total *dex1* chromosomal DNA was partially digested with *Sau*3A and size fractionated. Fragments greater than 14 kb were ligated into dephosphorylated *Bam*HI arms of λGEM11, packaged, and amplified in *Escherichia coli* KW251. Four clones that cross hybridized with T-DNA LB were isolated and characterized by restriction mapping and Southern analysis. One clone contained a 2.7-kb *Hin*dIII/*Eco*RI fragment adjacent to LB. The other clone contained a 3.0-kb *Sac*I fragment composed of genomic plant DNA and LB sequences.

Wild-type DNA corresponding to the T-DNA insertion site in *dex1* plants was isolated from an Arabidopsis (Columbia ecotype) genomic library constructed in λ-GEM11 (a gift from Dr. Elliot Meyerowitz, California Institute of Technology, Pasadena) using the 2.7-kb *Hin*dIII/*Eco*RI and 3.0-kb *Sac*I subclones as probes. Three positive clones were isolated and characterized by restriction mapping and Southern-blot analysis. Two clones were identical and overlapped with the third clone by 4.5 kb.

The 2.7-kb *Hin*dIII/*Eco*RI and 3.0 kb *Sac*I subclones were used to screen the PRL-2 cDNA library (a gift from Chris Somerville, Carnegie Institute of Washington, Stanford, CA). A 1,938-bp, partial-length cDNA that mapped to both sides of the T-DNA insertion site was isolated. Genomic and cDNA clones were subcloned and sequenced (Sanger et al., 1977). All regions of a 7.4-kb genomic region were sequenced on both strands at least one time. Analyses of DNA sequences were conducted using DNASTAR software (DNASTAR, Inc., Madison, WI). Potential exons in the genomic DNA were identified by NetPlantGene version 1.0b (http://www.cbs.dtu.dk/services/NetPGene; Hebsgaard et al., 1996). Intron and exon boundaries were identified by comparing genomic (accession no. AF257186) and cDNA (accession no. AF257187) sequences. BLAST searches were used to identify homologous sequences.

Isolation of the 5′ End of the DEX1 cDNA

The 5′ end of the *DEX1* cDNA was isolated using RT-PCR and IPCR. Primers (Fig. 2B) corresponding to predicted exon sequences were used for reverse transcription and PCR amplification on total bud RNA purified by LiCl precipitation. Reverse transcription with primer BIBe followed by PCR amplification using BIBen and either the DP-3–4.5 or DP-Xho primers resulted in an additional 484 and 465 bp of *DEX1* cDNA, respectively. IPCR (Zeiner and Gehring, 1994) was used to obtain the 5′ end of the cDNA. The gene-specific primer cDP-2610 was used for reverse transcription followed by second-strand synthesis and ligation. The ligation products were subjected to PCR with primers cDP-2350 and cDP-2595. All fragments were blunt-end cloned into pBlueScript, and 18 clones were analyzed by sequence analysis.

Complementation Construct and Plant Infiltration

A 10-kbp genomic DNA fragment spanning the T-DNA insertion site (Fig. 2A) was cloned into the binary vector pPZP121 (Hajdukiewicz et al., 1994) and introduced to *Agrobacterium tumefaciens* EHA105 using electroporation (Mersereau et al., 1990). The resulting strain was used to

transform a segregating population of *dex1* plants by vacuum infiltration. Seeds were harvested from infiltrated plants and plated on Murashige and Skoog plates containing 100 of μg mL^{-1} gentamycin. Thirty resistant seedlings were transferred to soil and allowed to self-fertilize. Seeds were collected from individual plants and sown onto Murashige and Skoog kanamycin plates to check for the presence of the T-DNA insert. Seven lines segregated for kanamycin; two lines were completely resistant. Resistant seedlings were scored for fertility/sterility. PCR was conducted on the homozygous kanamycin-resistant lines to confirm that fertile plants contained the gentamycin resistance gene.

ACKNOWLEDGMENTS

We are grateful to Xue Cai and Richard Edelmann for help with photography and image analysis and the Miami University Electron Microscopy Facility (Oxford, OH) for use of the rapid-freezing equipment, ultramicrotome, and transmission electron microscope.

Received June 13, 2001; returned for revision August 6, 2001; accepted August 25, 2001.

LITERATURE CITED

Ahlers F, Thom I, Lambert J, Kuckuk R, Wiermann R (1999) H-1 NMR analysis of sporopollenin from *Typha angustifolia*. Phytochemistry **5:** 1095–1098

An Y, McDowell JM, Huang S, McKinney EC, Chambliss S, Meagher RB (1996) Strong, constitutive expression of the *Arabidopsis ACT2/ACT8* actin subclass in vegetative tissues. Plant J **1:** 107–121

Blackmore S, Barnes S (1990) Pollen wall development in angiosperms. *In* S Blackmore, RB Knox, eds, Microspores: Evolution and Ontogeny. Academic Press, London, pp 173–192

Brett C, Waldron K (1990) Physiology and biochemistry of plant cell walls. *In* M Black, J Chapman, eds, Topics in Plant Physiology 2. Unwin Hyman, Inc., London, pp 72–127

Cutter EG (1971) Plant Anatomy: Experiment and Interpretation. Addison-Wesley, Reading, MA

Dickinson HG, Heslop-Harrison J (1977) Ribosomes, membranes and organelles during meiosis in angiosperms. Philos Trans R Soc Lond Biol **277:** 327–342

Dickinson HG, Sheldon JM (1986) The generation of patterning at the plasma membrane of the young microspore of *Lilium*. *In* S Blackmore, IK Ferguson, eds, Pollen and Spores: Form and Function. Academic Press, London, pp 1–17

Doyle J, Doyle J (1990) Isolation of plant DNA from fresh tissue. BRL Focus **12:** 13–15

El-Ghazaly G, Moate R, Cresti M, Walles B, Takahashi Y, Ferreira F, Obermeyer G (1999) Localization and release of allergens from tapetum and pollen grains of *Betula pendula*. Protoplasma **208:** 37–46

Erdtman G (1952) Pollen Morphology and Plant Taxonomy: An Introduction to Palynology. Almqvist & Wiksell, Stockholm

Erdtman G (1969) Handbook of Palynology: An Introduction to the Study of Pollen Grains and Spores. Hafner Publishing Co, New York

Feldmann KA, Marks MD (1987) *Agrobacterium*-mediated transformation of germinating seeds of *Arabidopsis thaliana*: a non-tissue culture approach. Mol Gen Genet **208:** 1–9

Fitzgerald MA, Knox RB (1995) Initiation of primexine in freeze-substituted microspores of *Brassica campestris*. Sex Plant Reprod **8:** 99–104

Futterer J, Hohn T (1996) Translation in plants: rules and exceptions. Plant Mol Biol **32:** 159–189

Hajdukiewicz P, Svab Z, Maliga P (1994) The small, versatile *pPZP* family of *Agrobacterium* binary vectors for plant transformation. Plant Mol Biol **25:** 989–994

Hebsgaard SM, Korning PG, Tolstrup N, Engelbrecht J, Rouze P, Brunak S (1996) Splice site prediction in *Arabidopsis thaliana* DNA by combining local and global sequence information. Nucleic Acids Res **24:** 3439–3452

Heslop-Harrison J (1963) An ultrastructural study of pollen wall ontogeny in *Silene pendula*. Grana Palynologica **4:** 7–24

Heslop-Harrison J (1971a) The pollen wall: structure and development. *In* J Heslop-Harrison, ed, Pollen: Development and Physiology. Butterworth, London, pp 75–98

Heslop-Harrison J (1971b) Wall pattern formation in angiosperm microsporogenesis. Symp Soc Exp Biol **25:** 277–300

Heslop-Harrison J (1976) The adaptive significance of the exine. *In* IK Ferguson, J Muller, eds, The Evolutionary Significance of the Exine. Academic Press, New York, pp 27–38

Hoefert LL (1968) Polychromatic stains for the thin sections of *Beta* embedded in epoxy resin. Stain Technol **43:** 145–151

Horton P, Nakai K (1996) A probabilistic classification system for predicting the cellular localization sites of proteins. Intellig Syst Mol Biol **4:** 109–119

Jacobson A (1987) Purification and fractionation of poly(A)+ RNA. Methods Enzymol **152:** 254–261

Jofuku KD, den Boer BGW, Van Montagu M, Okamuro JK (1994) Control of *Arabidopsis* flower and seed development by the homeotic gene *APETALA2*. Plant Cell **6:** 1211–1225

Joshi CP, Zhou H, Huang X, Chiang VL (1997) Context sequences of translation initiation codons in plants. Plant Mol Biol **35:** 993–1001

Kiss JZ, Giddings TH, Staehelin LA, Sack FD (1990) Comparison of the ultrastructure of conventionally fixed and high pressure frozen/freeze substituted root tips of *Nicotiana* and *Arabidopsis*. Protoplasma **157:** 64–74

Kiss JZ, Staehelin LA (1995) High pressure freezing. *In* NJ Severs, DM Shotton, eds, Rapid Freezing, Freeze Fracture and Deep Etching. Wiley-Liss, New York, pp 89–104

Klucher KM, Chow H, Reiser L, Fischer RL (1996) The *AINTEGUMENTA* gene of *Arabidopsis* required for ovule and female gametophyte development is related to the floral homeotic gene *APETALA2*. Plant Cell **8:** 137–153

Knox RB, Suphioglu C (1996) Pollen allergens: development and function. Sex Plant Reprod **9:** 318–323

Kudlicka K, Brown R (1997) Cellulose and callose biosynthesis in higher plants: I. Solubilization and separation of (1->3)- and (1->4)-beta-glucan synthase activities from mung bean. Plant Physiol **115:** 643–656

Logemann J, Schnell J, Willmitzer L (1987) Improved method for the isolation of RNA from plant tissue. Anal Biochem **163:** 16–20

Lukaszewicz M, Jerouville B, Boutry M (1998) Signs of translational regulation within the transcript leader of a plant plasma membrane H^+-ATPase gene. Plant J **14:** 413–423

Makaroff CA, Palmer JD (1987) Extensive mitochondrial specific transcription of the *Brassica campestris* mitochondrial genome. Nucleic Acids Res **15:** 5141–5156

Memelink J, Swords KMM, de Kam RJ, Schilperoort RA, Hoge HC, Staehelin LA (1993) Structure and regulation of tobacco extensin. Plant J **4:** 1011–1022

Mersereau M, Pazour GJ, Das A (1990) Efficient transformation of *Agrobacterium tumifaciens* by electroporation. Gene **90:** 149–151

Meuter-Gerhards A, Riegart S, Wiermann R (1999) Studies on sporopollenin biosynthesis in *Curcurbita maxima* (DUCH)-II: the involvement of aliphatic metabolism. J Plant Physiol **154:** 431–436

Morris PC, Guerrier D, Leung J, Giraudat J (1997) Cloning and characterization of MEK1, an *Arabidopsis* gene encoding a homologue of MAP kinase. Plant Mol Biol **35:** 1057–1064

Murashige T, Skoog F (1962) A revised medium for rapid growth and bioassays with tobacco tissue culture. Physiol Plant **15:** 493–497

Nasrallah JB, Nasrallah ME (1989) The molecular genetics of self-incompatibility in *Brassica*. Ann Rev Genet **23:** 121–139

Owen HA, Makaroff CA (1995) Ultrastructure of microsporogenesis and microgametogenesis in *Arabidopsis thaliana* (L.) Heynh. ecotype Wassilewskija (*Brassicaceae*). Protoplasma **185:** 7–21

Palmer EL, Ruegg C, Ferrando R, Pytela R, Sheppard D (1993) Sequence and tissue distribution of the integrin alpha9 subunit, a novel partner of beta1 that is widely distributed in epithelia and muscle. J Cell Biol **123:** 1289–1297

Paxson-Sowders DM, Owen HA, Makaroff CA (1997) A comparative ultrastructural analysis of exine pattern development in wild-type *Arabidopsis* and a mutant defective in pattern formation. Protoplasma **198:** 53–65

Peirson BN, Owen HA, Feldmann KA, Makaroff CA (1996) Characterization of three male-sterile mutants of *Arabidopsis thaliana* exhibiting alterations in meiosis. Sex Plant Reprod **9:** 1–16

Perez-Munoz CA, Webster BD, Jernstedt JA (1995) Spatial congruence between exine pattern, microtubules and endomembranes in *Vigna* pollen. Sex Plant Reprod **8:** 147–151

Reiser L, Modrusan Z, Margossian L, Samach A, Ohad N, Haughn GW, Fischer RL (1995) The *BELL1* gene encodes a homeodomain protein involved in pattern formation in the *Arabidopsis* ovule primordium. Cell **83:** 734–742

Rowley JR, Skvarla JJ (1975) The glycocalyx and initiation of exine spinules on microspores of *Canna*. Am J Bot **62:** 479–485

Rowley JR, Southworth D (1967) Deposition of sporopollenin on lamellae of unit membrane dimensions. Nature **213:** 703–704

Sanger F, Nicklen S, Coulson AR (1977) DNA sequencing with chain-terminating inhibitors. Proc Natl Acad Sci USA **74:** 5463–5467

Scott RJ (1994) Pollen exine: the sporopollenin enigma and the physics of pattern. *In* RJ Scott, MA Stead, eds, Molecular and Cellular Aspects of Plant Reproduction. University Press, Cambridge, UK, pp 49–81

Sheldon JM, Dickinson HG (1983) Determination of patterning in the pollen wall of *Lilium henryi*. J Cell Sci **63:** 191–208

Skvarla JJ, Larson DA (1966) Fine structural studies of *Zea mays* pollen: I. Cell membranes and exine ontogeny. Am J Bot **53:** 1112–1125

Stanley RG, Linskens HF (1974) Pollen: Biology, Biochemistry, Management. Springer-Verlag, New York, pp 13–28

Takahashi M (1989) Pattern determination of the exine in *Caesalpinia japonica* (Leguminosae: Caesalpinioideae). Am J Bot **76:** 1615–1626

Takahashi M, Skvarla JJ (1991) Exine pattern formation by plasma membrane in *Bougainvillea spectabilis* (Nyctaginaceae). Am J Bot **78:** 1063–1069

Toriyama K, Hanaoka K, Okada T, Watanabe M (1998) Molecular cloning of a cDNA encoding a pollen extracellular protein as a potential source of a pollen allergen in *Brassica rapa*. FEBS Lett **424:** 234–238

Wu L, Ueda T, Messing J (1995) The formation of mRNA 3′-ends in plants. Plant J **8:** 323–329

Zeiner M, Gehring M (1994) Cloning of 5′ cDNA regions by inverse PCR. BioTechnology **17:** 1050–1054

Zinkl GM, Zwiebel BI, Grier DG, Preuss D (1999) Pollen-stigma adhesion in *Arabidopsis*: a species-specific interaction mediated by lipophilic molecules in the pollen exine. Development **126:** 5431–5440